Kinetic Pathways of Ion Pair Dissociation in Water

Phillip L. Geissler, Christoph Dellago, and David Chandler*

*Department of Chemistry, University of California, Berkeley, California 94720*

Received: December 31, 1998; In Final Form: February 18, 1999

We have successfully applied the transition path sampling method to the deterministic dynamics of a many-body system with long-ranged interactions. The process we investigate, dissociation of a model Na^+Cl^- ion pair in water, involves a wide range of transition pathways in which collective solvent motions play an important role. Transition states along these pathways encompass a broad distribution of ionic separations. Ion pairs in contact remain associated for ~20 ps on average, a time scale considerably longer than the ~3ps predicted by transition state theory with ionic separation as the order parameter. In contrast to theories of barrier crossing based upon frictional effects (with or without memory), we find that the discrepancy between these time scales arises from neglected solvent free energy barriers rather than stochastic buffeting of the ion pair.

I. Introduction

By mediating interactions between charged solutes, water influences the kinetics and thermodynamics of a wide variety of processes, ranging from simple chemical reactions to structural organization of proteins. On a coarse level, the aqueous environment of solvated ions functions as a polarizable medium which favors the separation of attracting charges. The molecular nature of water, however, can give rise to further solvation effects. The interplay between hydrogen bond energetics and packing effects at high densities gives rise to complex dynamics in which cooperative solvent motions can be important for transitions between stable states. Furthermore, a broad ensemble of transition states is expected to be accessible to a many-body system at finite temperature. A process such as ion pair dissociation can involve barrier crossing in the direction of collective coordinates that are not simple to locate or to characterize.

In models of aqueous Na^+Cl^- solution, water is known to play a nontrivial role in ion pair dissociation.[1−3] Kinetics studies show that an order parameter describing only the ionic separation, $r_{ion} \equiv |\mathbf{r}_{Na^+} - \mathbf{r}_{Cl^-}|$, does not provide an adequate description of transition dynamics at room temperature. Many trajectories which surmount the free energy barrier of ~2.5 $k_B T$ along this coordinate do not relax monotonically into a stable associated or dissociated state. Within the framework of multidimensional barrier crossing theory, this fact can be interpreted in two distinct ways. (For a comprehensive review of the theory of barrier crossing with friction, see ref 4.) In the first interpretation one supposes that the transition states for dissociation coincide with the free energy maximum along r_{ion}, as depicted in Figure 1a. The solvent then contributes a fluctuating force with zero mean to the dynamics of the ion pair, causing recrossing of the barrier $r_{ion} = r^*$. Alternatively, one can imagine that important solvent free energy barriers exist in directions orthogonal to r_{ion}, as depicted in Figure 1b. In this case many configurations atop the solute free energy barrier in fact belong to the basin of attraction of one of the stable states. Most recrossings in the direction of r_{ion} are then simply fluctuations within a stable state. In order to reach a true transition state, reorganization of water molecules around the ion pair is necessary. These two scenarios differ significantly in their implications for solvent participation in solute dynamics,
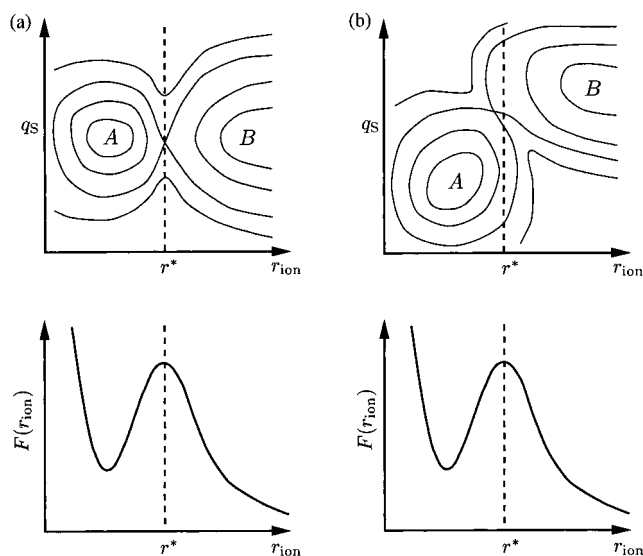
Figure 1. Two possible scenarios for ion pair dissociation in which a solvent coordinate q_S plays very different roles. The corresponding free energy landscapes $F(r_{ion}, q_S)$ are depicted in the upper two parts. The corresponding reduced free energies $F(r_{ion}) = -k_B T \ln \int dq_S \exp[-\beta F(r_{ion}, q_S)]$ are depicted in the lower two parts. For the free energy landscape depicted in part (a), the barrier separating stable associated (*A*) and dissociated (*B*) states is well-described by the ionic separation r_{ion}, and motion atop the barrier is predominantly in the direction of this solute coordinate. The maximum of the free energy $F(r_{ion})$ along r_{ion} coincides with the transition state for dissociation. A dividing surface defined by $r_{ion} = r^*$ therefore separates the basins of attraction for states A and B. For the landscape shown in part (b), however, motion over the barrier involves solvent reorganization described by q_S. Although the free energy $F(r_{ion})$ along r_{ion} may be identical to that for landscape part (a), the dividing surface $r_{ion} = r^*$ does not discriminate between the two stable states. Most configurations with $r_{ion} = r^*$ belong to one of the basins of attraction and not to the transition state region. Transitions between A and B require crossing a solvent free energy barrier orthogonal to the solute order parameter r_{ion}.

but conventional simulations do not allow one to distinguish between them.

In order to resolve the issue of solvent participation, it is necessary to collect a large number of properly weighted

Ion Pair Dissociation in Water

J. Phys. Chem. B, Vol. 103, No. 18, 1999 **3707**

dissociation trajectories and to analyze the transition states through which they pass. The transition path sampling method[5-7] provides algorithms for these purposes. In the present work we use transition path sampling to harvest deterministic dissociation pathways in a model of Na^+Cl^- in water. The model is described in section II. Rate constant calculations, presented in section III, demonstrate that there is no difficulty in applying transition path sampling to a many-body system in which long-ranged forces are important.

Using trajectories generated by path sampling, we construct an ensemble of transition states for dissociation. Configurations are classified by the probabilities of relaxing into the associated and dissociated states when momenta are assigned at random. If these probabilities are equal, a configuration is considered to be a transition state.[8,9] Analysis of distributions in the transition state ensemble, discussed in section IV, reveals that water plays an active role in ion pair dissociation. A wide distribution of the order parameter r_{ion} indicates that a variety of solvent reorganization pathways are indeed available for the transition. From solvent density distributions around the ion pair we determine the collective coordinates which help to drive dissociation. In particular, the number of water molecules in the first solvation shell of the Na^+ ion is an important quantity in these dynamics. Density fluctuations in the second and third solvation shells help promote this change in coordination number. Classification of configurations within the constrained ensemble $r_{ion} = r^*$, also discussed in section IV, aids in this analysis.

II. Model

For molecular dynamics simulations we consider a model similar to that of Guardia and co-workers.[2] The ion pair interacts through a Huggins—Mayer potential,[10] which includes short-ranged repulsion, Coulomb attraction, and dispersion. Water molecules interact according to the rigid TIP4P model.[11] Water—ion interactions include Coulomb and Lennard-Jones contributions.[10] Long-ranged Coulomb forces in the periodically replicated system are computed using Ewald summation.[12] The thermodynamic state of the microcanonical system was chosen using the ambient density of water and an energy corresponding to an average temperature of approximately 300 K.

For computational convenience it is desirable to use the smallest number of particles which reproduces the correct physics of the infinitely dilute system. To examine the effects of a finite simulation cell, we have computed the potential of mean force $w(r_{ion})$ between the two ions for systems with 106, 254, and 862 periodically replicated water molecules (corresponding to cell lengths of 15, 20, and 30 Å, respectively). $w(r_{ion})$ was obtained by integrating the average force measured in a series of constrained simulations in the same way as described in ref 2. The corresponding free energy,

$$F(r_{ion}) = w(r_{ion}) - 2 \ln (r_{ion}) \qquad (1)$$

is plotted in Figure 2. Our results for the three systems, averaged over ~100—500 ps of dynamics, are statistically indistinguishable. Because the essential thermodynamics of dissociation appears to be reproduced even by the smallest system, we use a system with 106 water molecules for all dynamics calculations.

III. Rate Constants

In order to demonstrate that the path sampling method correctly reproduces the distribution of transition pathways in a system of this complexity, we have compared the dissociation
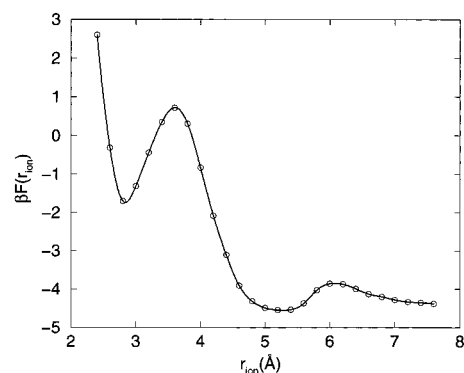
Figure 2. Free energy $F(r_{ion})$ of the aqueous Na^+Cl^- system as a function of ionic separation r_{ion} for a system with 106 water molecules in the central simulation cell. Along this coordinate a barrier of 2.5 k_BT separates the associated state from the local maximum of $F(r_{ion})$ at $r_{ion} = 3.6$ Å.

rate constant obtained from path sampling with that obtained from reactive flux calculations. Rate constants are computed from path sampling simulations by measuring the correlation $C(t)$ between stable state populations in time,[7]

$$C(t) \equiv \frac{\langle h_A[r_{ion}(0)]h_B[r_{ion}(t)]\rangle}{\langle h_A[r_{ion}(0)]\rangle} \qquad (2)$$

Here, angled brackets denote equilibrium averages over initial conditions, and the characteristic functions h_A and h_B define the associated and dissociated states, respectively. In this application, we take $h_A(r_{ion}) = 1$ for $r_{ion} < 3.2$ Å and $h_A(r_{ion}) = 0$ otherwise. Similarly, $h_B(r_{ion}) = 1$ for $r_{ion} > 4.4$ Å and $h_B(r_{ion}) = 0$ otherwise. With these choices the interionic separation r_{ion} serves well as an order parameter which distinguishes between the two stable states.

In essence, the correlation function given by eq 2 is the ratio of partition functions for two different ensembles of trajectories. The numerator is the partition function for trajectories which begin in state A and end in state B a time t later. Similarly, the denominator is the partition function for trajectories which begin in state A but with the final state of the system unconstrained. One can construct a continuum of ensembles between these two, for instance by varying the definition of state B. As such, $C(t)$ can be computed in effect by determining the reversible work to change between the two ensembles.[7] Using this perspective, we have computed $C(t)$ from tens of thousands of transition paths. The transition rate $\dot{C}(t)$ between the stable states, whose plateau value gives the phenomenological rate constant, is shown in Figure 3. After a transient time of about 1 ps, $\dot{C}(t)$ reaches a plateau with value 0.05 ps^{-1}. The corresponding characteristic time for dissociation is 20 ps.

For comparison we have performed reactive flux calculations, in which the reaction rate is measured more directly. The reactive flux,

$$k(t) \equiv \frac{\langle \dot{r}_{ion}\delta(r_{ion} - r^*)\theta[r_{ion}(t) - r^*]\rangle}{\langle \theta(r^* - r_{ion})\rangle} \qquad (3)$$

averages the flux crossing the surface $r_{ion} = r^*$ given that the product region is populated a time t later.[13,14] In eq 3, $\theta(x) = 1$ for $x > 0$ and zero otherwise. The separation $r^* = 3.6$ Å is the point of maximum free energy for the order parameter r_{ion}. Using standard methods,[13] we have computed $k(t)$ from 2000 trajectories originating at $r_{ion} = r^*$. The reactive flux is plotted alongside the path sampling result in Figure 3. The plateau value
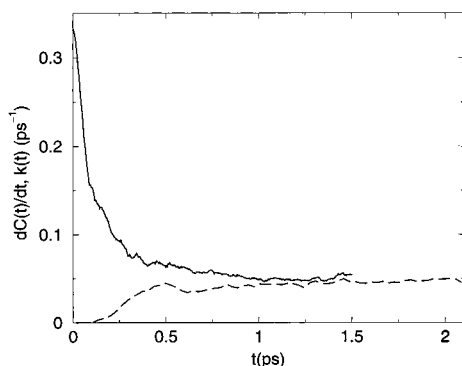
Figure 3. Transition rate $\dot{C}(t)$ (dashed) calculated in path sampling simulations and reactive flux $k(t)$ (solid line) as a function of time t. $\dot{C}(t)$ and $k(t)$ share the same asymptotic behavior after transient relaxation in the first picosecond. The plateau value 0.05 ps^{-1} corresponds to the dissociation rate constant. Statistical uncertainty for both calculations, estimated through block averages, is approximately 20%.
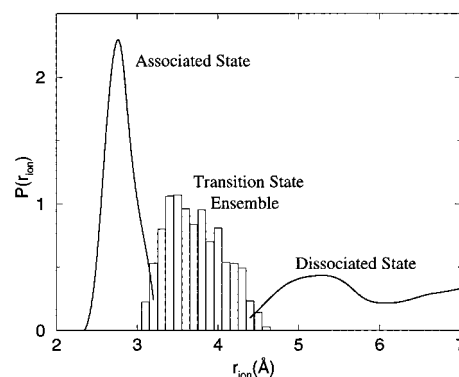

Figure 4. Distribution $P(r_{ion})$ of ionic separations in the stable associated and dissociated states, and in the transition state ensemble. Each distribution is normalized over the region shown.

Figure 5. Distribution $p(P_B)$ of the probability for relaxing to state B within the constrained ensemble $r_{ion} = r^*$. Values between 0 and 1 occur infrequently, indicating that most configurations are committed to one of the stable states. The distribution is consistent with a free energy difference of 1.7 $k_B T$ between the ensembles $P_B = 0$ and $P_B = 1/2$.

of $k(t)$ also gives the reaction rate constant.[14] The reaction time computed in this way is 20 ps. This result agrees with the path sampling result and compares well with previous reactive flux calculations on similar models.[1,2] Over the transient period, the reactive flux falls to less than 20% of its initial ($t = 0^+$) value. The initial value is the transition state theory estimate. The significant discrepancy between this transition state theory rate and the actual rate indicates that a large fraction of trajectories initiated at $r_{ion} = r^*$ will recross this dividing surface before relaxing into a stable state. Evidently, solvent motions play a significant role in the dissociation dynamics. Precisely how this role is played cannot, however, be ascertained from the implicit information provided by $k(t)$. Rather, explicit information is obtained from the ensemble of transition paths, as we now discuss.
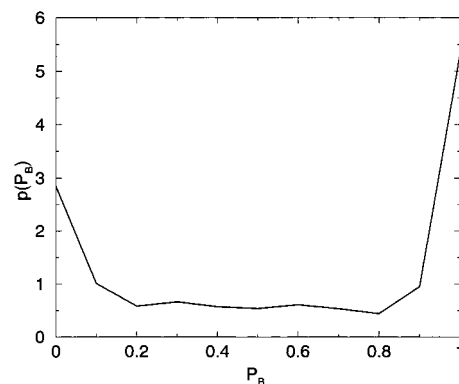
IV. Transition States

A. Transition State Ensemble. We have collected approximately 1000 members of the transition state ensemble by examining configurations along 750 statistically independent transition pathways. For each configuration along a path segment connecting the two stable states, we initiate a number of trajectories with momenta drawn randomly from a distribution consistent with the microcanonical ensemble. (Proper incorporation of constraints, such as rigid bonds, into the distribution of momenta is discussed in ref 15.) A transition state is identified if approximately half of these trajectories relax into each stable state after a transient time of 150 fs. In practice, we generate 10−100 trajectories to determine whether a configuration belongs to the transition state ensemble.

Distributions over the resulting collection of transition states reflect the wide variety of available dissociation pathways. As shown in Figure 4, transition states occur at a broad range of ionic separations, centered approximately at the free energy maximum $r_{ion} = r^*$. One even finds transition states at values of r_{ion} characteristic of the stable associated and dissociated states. This distribution suggests a cooperativity of transition dynamics in which the true reaction coordinate possesses a component orthogonal to the solute order parameter. However, this component is difficult to extract directly from the transition state ensemble due to the dispersion of configurations.

B. Solvent Behavior with Constrained Solute. In order to simplify the analysis of transition states, we have closely investigated 1000 configurations belonging to the constrained

ensemble with $r_{ion} = r^*$ (exactly the ensemble used for reactive flux calculations). In particular, we define a probability P_B for a given configuration as the fraction of trajectories initiated with random momenta which relax into stable state B. Since only two stable states are accessible in this system, the value of P_B indicates whether a configuration belongs to the basin of attraction of state A ($P_B = 0$) or state B ($P_B = 1$) or lies in an activated region between the basins of attraction ($P_B \approx 1/2$). The distribution of P_B within the constrained ensemble, shown in Figure 5, is remarkably revealing. The vast majority of configurations with $r_{ion} = r^*$ are committed to a stable associated or dissociated state. $P_B \approx 1/2$ for a very small percentage of configurations, so that $r_{ion} = r^*$ serves very poorly as a transition state criterion. This result indicates that the free energy landscape of this system resembles that in Figure 1b. A coordinate describing the state of the solvent is necessary to distinguish between the basins of attraction and to specify a transition state.

The observation that a solvent coordinate is required to locate transition states and the resulting distribution of P_B in the constrained ensemble are in sharp contrast with a simple picture of barrier crossing with friction. In such a simple picture, the ion pair interacts with an effective potential $w(r_{ion})$ and experiences a fluctuating force with zero mean (with or without memory). Because the stochastic force vanishes on average, this perspective predicts that $P_B \approx 1/2$ for any configuration atop the barrier $r_{ion} = r^*$. A narrow distribution of P_B centered about $P_B = 1/2$ is expected for this constrained ensemble. The distribution we have measured differs qualitatively, indicating

Ion Pair Dissociation in Water

J. Phys. Chem. B, Vol. 103, No. 18, 1999 **3709**
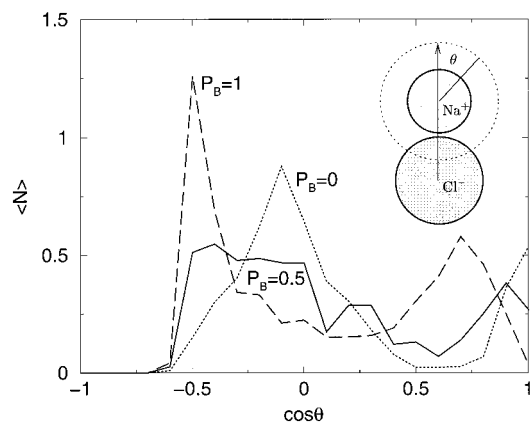
Figure 6. Angular distribution of water molecules in the first coordination shell of Na^+. The average number of water molecules $\langle N \rangle$ in angular bins is plotted as a function of the cosine of the polar angle θ for the subdivided constrained ensemble. Each angular bin has a width $\cos\theta = 0.1$. A water molecule is considered to be in the first coordination shell if the oxygen atom lies within 3.4 Å of the Na^+ ion.

that the simple picture is flawed. Guardia et. al.[2] and Dang et. al.[3] have used this one-dimensional picture of barrier crossing in applying Grote−Hynes theory[16] to this system. The rate constants they compute compare favorably with reactive flux calculations. Our results imply that the agreement they find is fortuitous.

The measured distribution of P_B also allows us to estimate the effect of solvent dynamics on phenomenological kinetics. The natural logarithm of the distribution gives a free energy along P_B in units of $k_B T$. Moving the system reversibly from $P_B = 0$ to $P_B = 1/2$ while maintaining the constraint $r_{ion} = r^*$ requires an amount of work $\ln(2.8/0.5)$ $k_B T = 1.7$ $k_B T$. This free energy barrier accounts almost quantitatively for the observed error in the one-dimensional transition state theory rate constant. It is the barrier to solvent reorganization rather than buffeting of the ion pair which is responsible for the error.

More importantly, this classification provides insight into the origin of the solvent free energy barrier. We have examined structural features of the solvent for constrained ensemble configurations with $P_B = 0$, $P_B = 1$, and $0.4 < P_B < 0.6$. The outstanding differences between these subensembles lie in the first coordination shell of the Na^+ ion. In over 80% of configurations, the Na^+ ion is five-fold coordinated when $P_B = 0$ and six-fold coordinated when $P_B = 1$. No such striking effect is found for the Cl^- ion, whose coordinating water molecules are more labile. It is clear that during the course of dissociation the coordination number of the Na^+ ion must increase from values typical in the associated state (from 3 to 5) to values typical in the dissociated state (from 6 to 7). However, it is a subtle fact that the addition of water molecules to the first solvation shell is a driving force for dissociation dynamics.

The mechanism for water addition to the Na^+ coordination shell is elucidated by further examination of these subensembles. In configurations with $P_B \approx 1/2$, the Na^+ ion is typically only five-fold coordinated. We therefore expect that at the transition state density rearrangements near the ion have activated the system for addition. Distribution of water molecules in the first coordination shell, shown in Figure 6, reveal that this expectation is correct. In reaching the transition state from the associated state, water molecules coordinating the Na^+ ion shift towards the Cl^- ion, freeing space for the incoming molecule. Creation of this gap in the highly ordered coordination shell costs roughly 1.7 $k_B T$.
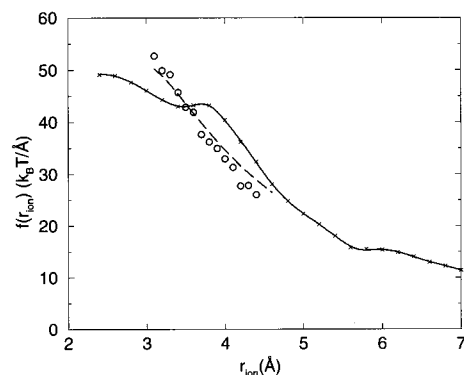
Figure 7. Mean solvent force $f(r_{ion})$ on the ion pair along the interionic axis as a function of ionic separation r_{ion}. The equilibrium average (solid line) and transition state ensemble average (circles) are shown alongside the negative of the direct interionic force (dashed line).

C. Solvent Structure in the Transition State Ensemble. With this insight into solvent behavior at a fixed ionic separation, we return to the analysis of the full transition state ensemble. It is not surprising that the interionic separation is correlated with progress of changing Na^+ ion coordination. Transition states with small values of r_{ion} have coordination shell structure resembling the dissociated state. Most have six-fold coordination of the Na^+ ion or a coordinating water distribution shifted in preparation for addition. By contrast, transition states with large r_{ion} resemble the associated state with five-fold coordination of Na^+. These observations are consistent with the free energy landscape sketched in Figure 1b with the appropriate solvent coordinate q_S describing coordination of the Na^+ ion.

Solvent structure in the transition state ensemble also provides evidence that density reorganization at longer length scales influences dissociation dynamics. The radial distribution of solvent molecules in a cone about the Na^+ ion shows that density fluctuations in the second and third solvation shells couple to the transition. Compared to configurations in the constrained ensemble, these transition states display on average an accretion of water density in the second solvation shell and a depletion between the second and third shells. The density buildup around 4 Å is likely associated with introduction of a "bulk" solvent molecule into the first coordination shell. It is reasonable to infer that the density depletion around 6 Å, which integrates to a single water molecule, provides space for the ion pair to separate. This molecule-sized void was not detected for each transition state, but transition states are more likely to occur when it is present.

The long range of solvent−solute interactions in this system gives rise to correlations in the transition state ensemble at long length scales as well. We measure this influence through the average solvent force on the solute, which contains contributions from all length scales. As shown in Figure 7, the component of this force along the interionic axis differs noticeably from the equilibrium result. The mean solvent force in the transition state ensemble cancels the direct interionic force almost exactly over a wide range of separations. The net force separating the ions therefore vanishes on average in the transition state ensemble, removing the instantaneous bias for the ion pair to relax towards one of the stable states. However, fluctuations in the solvent force are quite large (~ 10 $k_B T/Å$), so that a vanishing force does not by itself specify the ensemble of transition states.

V. Conclusions

We have demonstrated that path sampling can be used to extract subtle mechanistic details of transition dynamics in a

complex, many-body system with long-ranged interactions. For an ion pair in water, we find that the molecular nature of the solvent is important for dissociation dynamics. The free energy barrier for rearrangement of water molecules near the ion pair is comparable to that for separation of the ions. Consequently, the solvent does not relax rapidly on the time scale of solute motions, and it is not well-represented by a Gaussian bath as in standard frictional theories. The reaction coordinate for dissociation must include solvent as well as solute degrees of freedom. Specifically, incorporation of a sixth water molecule into the coordination shell of the Na^+ ion is necessary for dissociation and requires crossing a barrier of about 1.7 k_BT. In the corresponding transition state ensemble, the first solvation shell creates space for the incoming solvent molecule and density builds up in the second solvation shell. A molecular void between the second and third solvation shells facilitates these rearrangements.

The dynamical picture we have developed has implications for many processes involving ion chemistry in water. For small solvated ions we have shown that the time scales for relevant solvent rearrangement compare with time scales for interesting solute dynamics. It is therefore quantitatively important to account for explicit solvent dynamics. For large solutes there can be even longer time scales for solvent reorganization, further increasing the influence of solvent dynamics on solute kinetics.

References and Notes

(1) Berkowitz, M.; Karim, O. A.; McCammon, J. A.; Rossky, P. J. *Chem. Phys. Lett.* **1984**, *105*, 577. Belch, A. C.; Berkowitz, M.; McCammon, J. A. *J. Am. Chem. Soc.* **1986**, *108*, 1755. Karim, O. A.; McCammon, J. A.; *J. Am. Chem. Soc.* **1986**, *108*, 1762; Karim, O. A.; McCammon, J. A. *Chem. Phys. Lett.* **1986**, *132*, 219; McCammon, J. A.; Karim, O. A.; Lybrand, T. P.; Wong, C. F. *Ann. N.Y. Acad. Sci.* **1986**, *482*, 210.

(2) Rey R.; Guardia, E. *J. Phys. Chem.* **1992**, *96*, 4712; Guardia, E.; Rey, R. Padró, J. A. *Chem. Phys.* **1991**, *155*, 187; Rey, R.; Guardia, E.; Padró, J. A. *J. Chem. Phys.* **1992**, *97*, 1343.

(3) Smith, D. E.; Dang, L. X. *J. Chem. Phys.* **1994**, *100*, 3757.

(4) Hänggi, P.; Talkner, P.; Borkovec, M. *Rev. Mod. Phys.* **1990**, *62*, 251.

(5) Dellago, C.; Bolhuis, P. G.; Csajka, F. S.; Chandler, D. *J. Chem. Phys.* **1998**, *108*, 1964.

(6) Bolhuis, P. G.; Dellago, C.; Chandler, D. *Faraday Discussions* **1998**, *110*, 421.

(7) Dellago, C.; Bolhuis, P. G.; Chandler, D. *J. Chem. Phys.* **1999**, *110*, 6617.

(8) Klosek, M. M.; Matkowsky, B. J.; Schuss, Z. *Ber. Bunsen-Ges. Phys. Chem.* **1991**, *95*, 331.

(9) Pande, V.; Grosberg, A. Y.; Tanaka, T.; Shakhnovich, E. S. *J. Chem. Phys.* **1998**, *108*, 334.

(10) Pettit, B. M.; Rossky, P. J. *J. Chem. Phys* **1986***, 84*, 5836.

(11) Jorgenson, W. L.; Chandrasekhar, J.; Impey, R. W.; Klein, M. L. *J. Chem. Phys.* **1983**, *79*, 926.

(12) de Leeuw, S. W.; Perram, J. W.; Smith, E. R. *Proc. R. Soc. London* **1980**, *373*, 27.

(13) Chandler, D. *J. Chem. Phys.* **1978**, *68*, 2959.

(14) Chandler, D. *Introduction to Modern Statistical Mechanics*; Oxford University Press: New York, 1987.

(15) Geissler, P. L.; Dellago, C.; Chandler, D. *Phys. Chem. Chem. Phys.* **1999**, *1*, 1317.

(16) Grote, R. F.; Hynes, J. T. *J. Chem. Phys.* **1980**, *73*, 2715.